Electric appliance parts classification using a measure combining the whole shape and local shape distribution similarities

Ryo Hanai Kimitoshi Yamazaki Hiroaki Yaguchi Kei Okada
Masayuki Inaba
The University of Tokyo
7-3-1, Hongo, Bunkyo, Tokyo 113-8656, Japan
hanai,yamazaki,h-yaguchi,k-okada,inaba@jsk.t.u-tokyo.ac.jp

Abstract

Classification of electric appliance parts is one of the interesting and practically valuable applications for 3D object recognition. Based on existing works, in this paper we try classifying electric appliance parts data obtained in an automatable process, which becomes a basis for automated recycling system. The dataset includes deformable objects such as cables as well as various rigid objects, some of which lacking a large part of the surface because of self-occlusions and materials of the parts. To realize high accuracy in classification, after the comparison of several similarity measures, we combine a measure which describes well the whole shape similarity with a measure that expresses the ratio of local surface patterns that appears in each model. The latter measure is suitable to describe the similarity of deformable objects that the whole shapes are heavily dependent on their configurations. We also investigate how the scale of computing local feature affects the classification result.

1. Introduction

By the development of 3D measurement technology and algorithms for object recognition, the similarity of 3D geometry is becoming a powerful tool to classify objects in the real environment. On the other hand, automatic classification of electric appliance parts is expected for recycling.

In this paper, we consider the problem of classifying several hundreds of real electric appliance parts shown in Fig.1. The data includes deformable objects such as cables as well as rigid bodies, for example motors, circuit boards, small metal parts and screws. The data lacks a lot of faces because of self-occlusions and materials of the parts such as glasses. The shape variation in each class is smaller than that of usual 3D shape retrieval benchmarks but this is not the problem of identifying known objects under some uniform or artificial noise.

In this settings, the purpose of the paper is to find a feature and similarity measure suitable to classify the electric appliance parts.

2. Similarity based on 3D geometry

The problem of classification based on the 3D geometry of objects has been becoming important in the field of 3D information retrieval and 3D object recognition.

Density-based Framework(DBF)[1] is a technique that expresses the distribution of local surface features such as normals as a density function via kernel density estimation. This makes the feature insensitive to small shape perturbations and mesh resolution. CRSP[10] expresses a view from the center of a given model as a set of spherical functions and generate a feature vector with spherical harmonics transform. LFD[2] uses visual similarity from different views. The combination of several different features are found to increase the performance of information retrieval. These methods captures different aspects of similarity.

On the other hand, in the 3D model recognition, methods that are robust to noises or identifying object from a part of the shape which often caused by occlusions in real scenes are often focused. Some methods for image-based recognition are also applied to 3D geometry. Bag-of-features or bag-of-words is first introduced in the context of document retrieval. This approach expresses each document as a histogram of word frequency by ignoring the position each word appears. Then it is applied to object recognition from images by quantizing the local features extracted from images[4]. In 3D model retrieval, [8] employed bag-of-feature approach using spin image[6] as local feature, and [5] applied bag-of-feature based on SIFT[9] to depth images obtained by rendering 3D models. Surflet pair relation histogram[15] describes a relation between a pair of surface and its normals using four parameters and they are binned into a histogram. This feature has a benefit that it is rota-

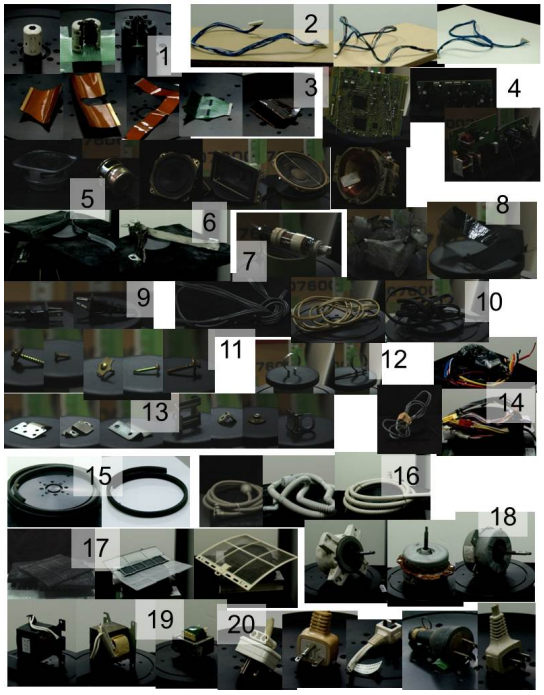

Figure 1. Dataset of electric appliance parts. The numbers in the figure shows the class each parts belongs to (362 parts, 20 classes).

tion invariant. [7] also proposed another rotation invariant feature by extending the information of the power spectrum of spherical harmonics using symmetry. [12] computed this feature locally and saliency of the local feature. Many applications need to evaluate similarity of 3D geometry. For example, point feature histogram[11] computed SPRH around each point to detect uniqueness in a given point cloud and consistency over scales for registration of scans.

Based on these works, we start with comparing several features. Then by introducing the feature focusing on the local geometry, we improve the classification accuracy for deformable objects. To compute the local features, there are two options: computing around uniformly sampled point or computing the feature only around points that are salient in some measures. We use the first approach because the variation of local surface patterns of electric appliance parts are small compared with natural objects such as dragons often used in object recognition examples. Then we improve further by combining the global shape similarity and the distribution of local surface patterns.

The rest of the paper is organized as follows. In the next section, we present the dataset of electric appliance parts. Then Section 4 compares features to describe the whole shape of input models. A measure suitable to deformable objects is introduced in Section 5. After that Section 6 shows that a better measure for electric appliance parts data is realized by combining the whole shape similarity and the

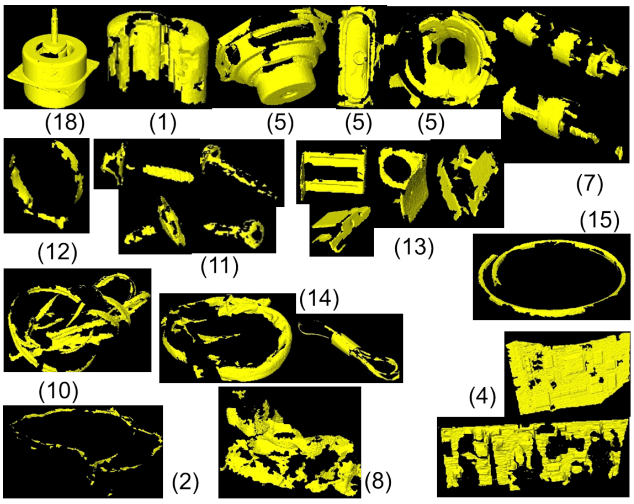

Figure 2. 3D models acquired with VIVID910. The numbers in the figure shows the class number.

local shape distribution similarity. Finally, Section 7 concludes this paper.

3. Dataset of electric appliance parts

This section describes our dataset in detail. We used VIVID910 by Konica Minolta Co.,Ltd. to measure electric parts. The absolute accuracy of VIVID910 is $X : \pm 0.22[mm]$, $Y : \pm 0.16[mm]$, $Z : \pm 0.10[mm]$ in fine mode and its relative accuracy is $\pm 0.008[mm]$ in high reliability mode by the specification. Absolute accuracy means the error of positions between measuring equipment and a target object to be measured. Relative accuracy is the error of relative positions between measured points. Therefore, the accuracy of the acquired models depends on the relative accuracy. The parts were measured from several different views by rotating on a turn table, and the data was integrated with software attached to VIVID910. The format of the model is polygon with normals. This measurement process is valid as a setting for future automation of the classification task in that it does not require data modification processes by hand. The dataset consists of 362 models and classified into 20 classes. Table 1 shows the number of models in each class. After the measurement and integration of scans, the polygons are reduced using the tool attached to VIVID, since the size of raw data is large. Therefore, their accuracy is lower than that of VIVID itself.

Fig.2 shows some of measured models. The number in the picture shows the class to which each parts belongs. This corresponds to the number in Fig.1. The quality of acquired models heavily depends on the parts. Generally, the models of comparatively large rigid objects with convex-like shapes are clean. Examples are (18),(1) and (5), though

Class no.	Number of models
16,17	5
6,18,19	10
14	13
11,12	19
1,4,9,13,15	20
20	21
2,7	22
5	30
8	37
3	39

Table 1. The number of models in each class of the dataset.

some part of surface is missing. Electron guns (7) have a cylindrical shape, but glass material on their side is not detected by laser, resulting in considerably chipped models. Small metal parts such as screws (11) are difficult to get the whole clean shape. Deformable objects such as cables ((10),(14),(15),(2) and (8)) also lack lots of faces because of occlusions caused by their complex configurations. The situation is really bad when the cables are very thin. Cables are separated into several classes depending on their usages. Circuit boards are basically flat, but have small difference on parts on the board. When the parts on the boards are large, some holes occur in the measured data (4).

4. Similarity measure of the whole geometry

We start with comparing some features by applying them to our electric appliance parts dataset. There are many features to describe the similarity of 3D models. Akgul *et al.* gives a good survey and comparison[1]. From their comparison we chose DBF[1] and CRSP[10], which achieve high scores for several benchmark sets such as Princeton Shape Benchmark[13]. We also added SPRH to the candidates. This is introduced in the context of 3D object recognition. [15] showed this feature can cope with some amount of occlusions and uniformly distributed noise.

The measures to evaluate them are Discounted Cumulative Gain(DCG) and Nearest Neighbor(NN), which are often used in 3D model retrieval. NN is the percentage of the first-closest matches that belong to the query class. A high NN score indicates the potential of the algorithm in a classification application. DCG evaluates the entire sequence of the ordered objects by a similarity measure and gives larger weight to higher rank of corrects/incorrects. Therefore DCG is more suitable to compare the ability to describe classes in the dataset.

We applied above three methods to the whole electric appliance parts dataset. DBF is a framework that smoothes in feature space using kernel density estimation technique and there are several options for local features. In this experiment, we used a first-order feature that combines the

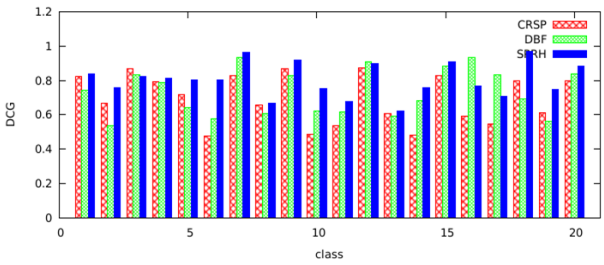

Figure 3. Comparison of DBF, CRSP and SPRH (DCG).

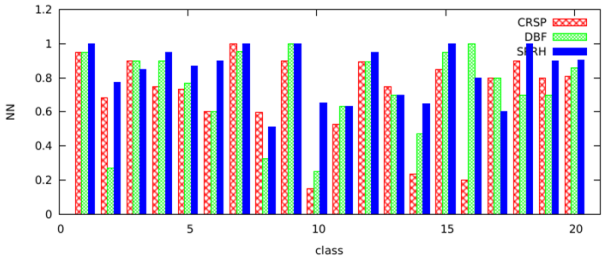

Figure 4. Comparison of DBF, CRSP and SPRH (NN).

normal direction and the radial-normal alignment. SPRH feature is computed after normalizing the size of the input models as the other two methods do. Fig.3 and Fig.4 show the score. The horizontal axis is the class number. It is found that SPRH is a good measure to even for models with not only random noise but some amount of missing surface in the models. In the experiment, SPRH outperformed the other two methods for most of the classes. One reason is that SPRH is rotation invariant. For some benchmarks, methods using alignment techniques such as continuous PCA[14] or PCA with respect to normals[10] show good results[1]. However, we have many models which are difficult to determine their base coordinates to be consistent in each class. The way surface lacks also affects the result of orientation alignment. Another reason is that SPRH utilizes information higher than second-order. To distinguish objects like cables, local curvatures are very effective. The other reason is that the electric appliance parts dataset has classes that are separated by small differences on plane-like objects and the difference in local curvatures rather that the similarity of the whole shape.

4.1. Surflet pair relation histograms (SPRH)

A pair of a surface and its normal is called surflet and [15] proposed SPRH feature by describing the relation between many pairs of surflets sampled from a model and binning into a histogram. For a given surflet pair $(\mathbf{p_1}, \mathbf{n_1}), (\mathbf{p_2}, \mathbf{n_2})$, First a coordinate system is defined. The origin is chosen to be $\mathbf{p_1}$, if

$$|\mathbf{n_1} \circ (\mathbf{p_2} - \mathbf{p_1})| \leq |\mathbf{n_2} \circ (\mathbf{p_2} - \mathbf{p_1})| \qquad (1)$$

and $\mathbf{p_2}$ otherwise so that the following base vectors are defined robustly. Then base vectors $\mathbf{u}, \mathbf{v}, \mathbf{w}$ are defined as

$$\mathbf{u} = \mathbf{n_1} \quad (2)$$

$$\mathbf{v} = \frac{(\mathbf{p_2} - \mathbf{p_1}) \times \mathbf{u}}{\|(\mathbf{p_2} - \mathbf{p_1}) \times \mathbf{u}\|} \quad (3)$$

$$\mathbf{w} = \mathbf{u} \times \mathbf{v} \quad (4)$$

Using these base vectors, the relation between two surflets are described by four parameters

$$\alpha = \arctan(\mathbf{w} \circ \mathbf{n_2}, \mathbf{u} \circ \mathbf{n_2}) \quad (5)$$

$$\beta = \mathbf{v} \circ \mathbf{n_2} \quad (6)$$

$$\gamma = \mathbf{u} \circ \frac{\mathbf{p_2} - \mathbf{p_1}}{\|\mathbf{p_2} - \mathbf{p_1}\|} \quad (7)$$

$$\delta = \|\mathbf{p_2} - \mathbf{p_1}\| \quad (8)$$

The two parameters are for relative positions excluding the DoF around the normal of base coordinates and the other two are for the relation between normal directions. SPRH features are given by quantizing these parameters and binning into a histogram. Since the histogram is computed over surflet pairs on the whole object, it includes information on global geometry as well as local geometry.

4.2. Poisson disk sampling over mesh

To compute SPRH feature, surflets need to be sampled from the input model. Using centroids of mesh is not good because the sizes of faces differ by more than two orders of magnitude. In [15], surflets are randomly sampled from the model. We use poisson disk sampling over mesh to get an expression free from the original mesh and cover the model uniformly with small number of samples, A poisson disk point set is a uniformly distributed set of points in which no two points are close to each other than some minimum distance r(Fig.7). In planes, by excluding the area known to be covered by existing samples, poisson disc point set is obtained efficiently using dart throwing algorithm [16]. Cline et al.[3] extended the target space of the dart throwing to various types of surfaces and showed experimentally that a large poisson disk point set can be generated on triangle meshes quickly. In their experiment, sampling of 10000 points took less than a second.

We use this to implement sampling over the input model. The normal of a surflet is that of a triangle where the point is sampled.

5. Similarity measure based on local shape distribution

SPRH feature shows good result for the electric appliance parts dataset (Fig.4). However, the score is comparatively low in classes of deformable objects such as class 2, 6, 8, 10 and 14. This result motivated us to introduce a measure that focuses more on the similarity of local geometry.

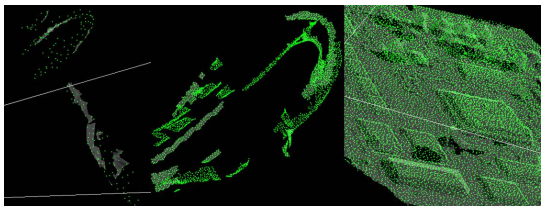

Figure 5. Sampling over mesh (r=1[mm], screw(left), cable(middle), surface of a circuit board(right))

The main difficulty in cables is that they change their configurations. However, being looked at in proper scales, they often show their uniqueness. This is because cables are not completely flexible objects such as cloth. They have cylindrical or flat feature around its axis in a small scale. The curvature along a cable axis is related to its thickness, material and the way it is used. The nice feature of cables is that they are uniform in the distribution of these local surface patterns. As a result, by describing cables focusing on this information, their similarity is defined in a robust manner against configuration changes as well as noise and the lack of surface caused by self occlusions.

5.1. Frequency of local surface patterns

Two typical approaches of choosing regions to compute local features are sampling salient regions in some measure and uniform sampling. Electric parts dataset is small in the variation of local surface pattern and salient point does not necessarily describe inherent feature of objects in the case of cables. For example, though points around knots of cables are salient, they are determined mainly by how they are placed. So we employ uniform sampling policy and describe models using the frequency of surface pattern. To generate a histogram from local features, so-called bag-of-words approach is used. That is we first compute local SPRH features for all the models in the dataset. After that they are divided into clusters using repeated bisectioning method[17]. Since this process is not the focus of this paper, we do not go further into it. These centroids of the clusters define a dictionary and we call the centroids *geowords*. Next, features extracted from each model are projected to the nearest geoword, generating a histogram of geowords for the model. Since we sample from the entire model uniformly, the above histogram expresses the model by the ratio of local surface patterns that appear in it.

5.2. Absolute scale vs. Relative scale

Most of the methods in the 3D model retrieval normalize the size of an input model at the first stage of feature extraction. One of the common approach is to normalize the

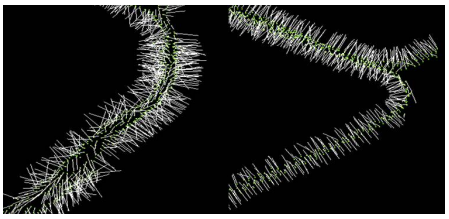

Figure 6. Normal vectors sampled over different types of cables (left:round,right flat).

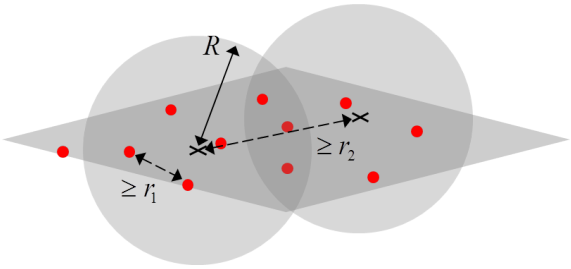

Figure 7. Sampling parameters. r is the constraint distance between sampling points. R defines the neighborhood within which local feature is computed.

model with respect to the area weighted distance to satisfy $(\sum_s S(s)d(s))/\sum_s S(s) = 1$, where $S(s)$ is the area of a face s and $d(s)$ is the distance from the origin to the center of the face. This is because models collected on the web are not equal in scale. Further the problem is often defined as *contents-based* classification, where objects of completely different size are considered to be in a same category if they have a same meaning. For example, a real car and a toy car are thought to be in the same class.

In the case of electric appliance parts, however, the absolute scale is rather important clue for classification. For example, what distinguishes cables are their width or local curvatures rather than the similarity of the whole shape. Knowing the object is in a cable class is not our objective. Certainly, some parts have similar global shape and differs in scale, but they do not necessarily scale isotropically, making the benefit of scale normalization small. In addition, the size of models are measured with high accuracy in our settings. Therefore we start the feature extraction process without rescaling input models.

5.3. Local feature extraction

This section describes the local feature extraction process in more detail. First, we apply poisson sampling to an input model using two minimum distances $r_1, r_2 (r_1 < r_2)$, and compute a local feature in each neighborhood of r_2 samples using dense samples of r_1. In each neighborhood, $4^4 = 256$ dimensions of SPRH features are computed. The local feature is computed by binning all pairs into the histogram in the neighborhood of radius R in the same manner as PFH[11] does(Fig.7). This means when 50 surflets exists in the neighborhood, 2500 pairs are binned into the histogram.

We choose 1[mm] as r_1 because it is small enough to preserve minute structures such as the difference of circuit board surface or difference of cable flatness and local geometry, which we want to utilize for classification(Fig.5). The resolution of the VIVID data is very high when the surface of an object is correctly detected. Although the accuracy reduces during the process of scan registration and following polygon reduction, information of 1[mm] scale is reliable to some extent in input models. Fig.6 shows the result of sampling from a round cable of 5[mm] radius and a flat cable of about 1[cm] of width. In the former case, there are various directions of normals. In the latter case, however, normals point to mainly two directions, showing the bias of the normal distribution. Basically in surface models, the number of points in the neighborhood of radius R is proportional to $(R/r)^2$, if they have plane-like surface and is close to R/r, if they are line-like surface. But since the number depends on the mesh in the neighborhood, we ignore neighbors that have less than 50 surflets from the computation of local features.

Next we computed SPRH by binning only relations of surflet pairs close to each other within a specified distance d(Fig.9) to investigate how much distant surface relations are informative for the classification of deformable objects. Table 2 shows the DCG scores for different d. From the figure, we can see that proper scale is dependent on the input objects. Classes 2 and 6 have different tendency from the other classes. This tendency can be said to be inherent feature of the cables in the classes, but this is also biased by the configurations of learning dataset. Most of the cables in class 2 are placed in comparatively simple configurations with less crossing. As a result, using distant surface relations helps identifying objects in class 2. In the later discussions, we use $R = 10$, which means surflet pairs within $20[mm]$ can be used.

class	2	6	8	10	14
d=10	0.841	0.857	0.867	0.950	0.815
d=20	0.894	0.886	0.858	0.916	0.808
d=40	0.904	0.910	0.796	0.857	0.800

Table 2. DCG scores of deformable object classes, when SPRH is built using pairs within distance d.

5.4. Experimental results

First, to confirm the hypothesis that cables are robustly separated in small scales, we computed geoword histograms in three scales using a set of parameters r and R. Fig.8 is the distribution of parts in the geoword space projected to 2D space using principal component analysis. Each point

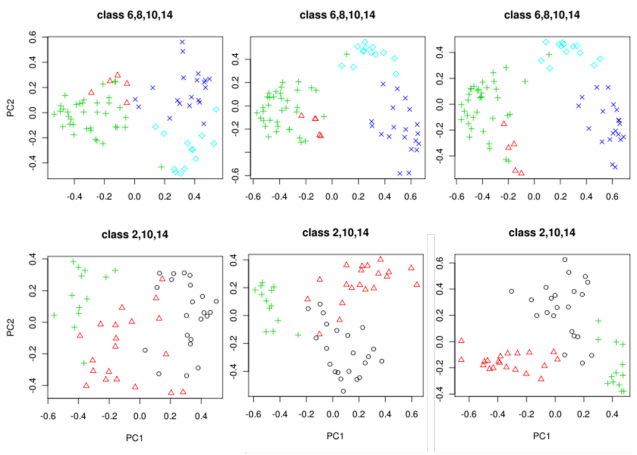

Figure 8. Distributions of deformable objects in geoword histogram space: The right column is the smallest scale. Clusters are separated in smaller scales. $(r, R) = (4, 40), (2, 20), (1, 10)[mm]$ from the left column.

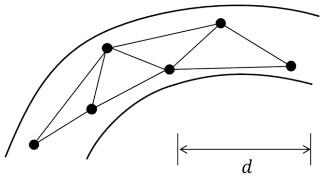

Figure 9. Surflet pairs within distance d are binned. Relations between distant pairs are not counted.

shows a corresponding parts. The left column is the largest scale and the right column is the smallest scale. The top row is the plot of deformable objects whose scores are low in Fig.4. The bottom row is the plot of similar round cables. We can see that classes form more separated clusters in smaller scales.

Then we make a comparison of SPRH feature computed over the whole shape and the distribution of local SPRH feature. We use L1 norm to evaluate the similarity between 2 geoword histograms. Fig.10 and Fig.11 show the result. As we expected, the local shape distribution performs well for deformable objects such as classes 8, 10 and 14. On the other hand, SPRH feature computed for the whole shape is more effective for some of rigid body objects especially in DCG. The two methods look working complementarily.

6. Combining features

From the consideration in the previous section, we can expect combining the benefits of global shape similarity and local shape distribution similarity and define a better similarity measure. One common approach to utilize different scales of information is extracting local features in several

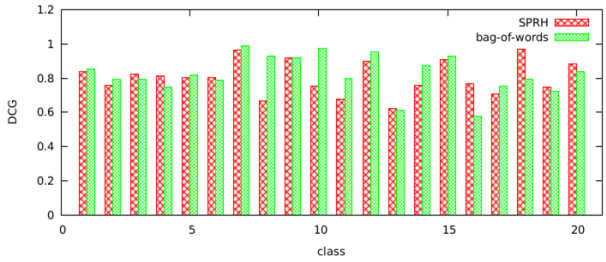

Figure 10. DCG, Comparison of SPRH for the whole shape and local surface pattern distribution (Bag-of-words)

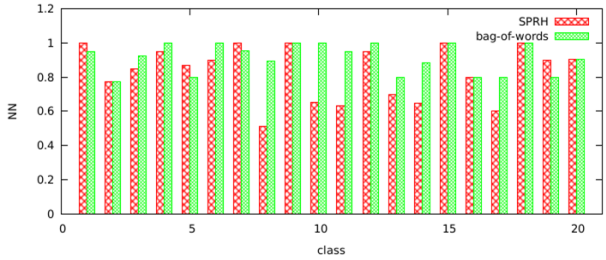

Figure 11. NN, Comparison of SPRH for the whole shape and local surface pattern distribution (Bag-of-words)

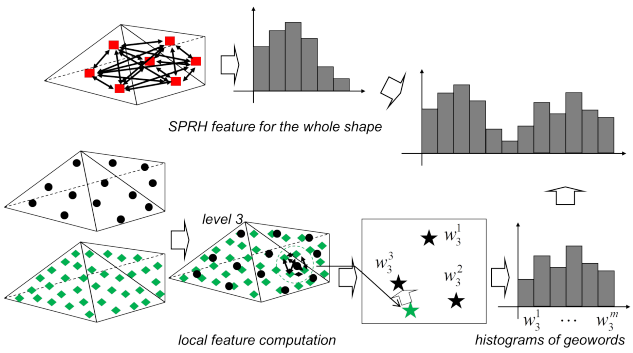

Figure 12. The computation flow of computing the combined feature.

scales. Large scale features capture the structure over large areas and small scale features capture high frequency structure over small regions. However, in our case, features computed for each scale are strongly correlated since the object is uniformly sampled and a region used in a scale is included in larger scales. Further, bag-of-words approach counts the number of features. In large scales, it is difficult to get a large number of local features and comparing the feature of the whole shape is more informative. Therefore we simply combine the above two feature vectors to directly compare SPRH feature for the whole shape. That is, after being normalized with respect to L1 norm, two different vectors are aligned. After that the combined whole vector is normalized again. This process is shown in Fig.12.

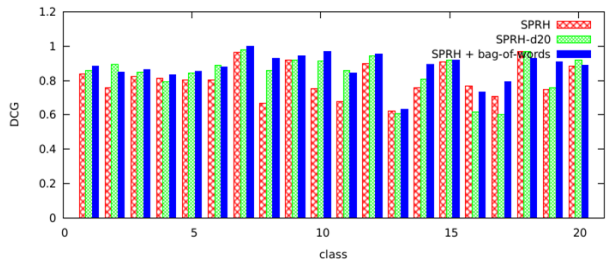

Figure 13. DCG, combined feature.

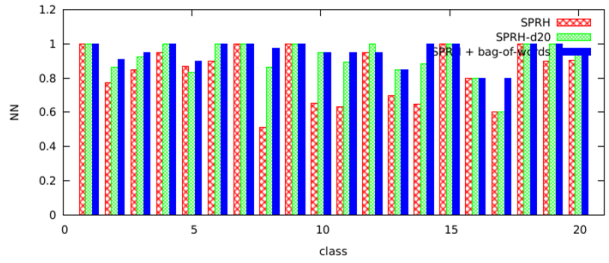

Figure 14. NN, combined feature.

Fig.13 and Fig.14 show the score. For comparison, the score of the combined vectors that use SPRH binned by relations of near surflets($d = 20[mm]$). Although the approach that uses near surflet relations improves the result of the whole shape SPRH largely, the combined measure using bag-of-words improves further. This is a simple combination of the two vectors, but the combined feature realizes as close as the better one between the whole shape SPRH and bag-of-words in most of the classes.

Table 3 summarizes the DCG and NN scores, which are shown as bar charts in Fig.3,Fig.4, Fig.10,Fig.11, Fig.13 and Fig.14. BoW in the figure means Bag-of-Words. The two DCG scores are scores averaged in for all parts in the dataset and scores once averaged within each class and further averaged among classes. The second scores have the same weight on each class regardless of the numbers of parts in the classes. NN(2nd) is the ratio when an object in the same class as query object appears within top 2nd rank of the list. We can see that generally high accuracy is achieved in spite of the quality of the dataset. This is a promising result as a first step toward an automated recycling system of electric appliance parts. Finally, some of the retrieval results of deformable objects are shown in . Even when the many faces are missing, deformable objects are retrieved correctly.

7. Conclusion

Classifying electric appliance parts is one of the interesting and practically valuable applications for 3D object recognition. This paper first presented a dataset of electric

feature	DCG(parts/class)	NN(1st/2nd)
CRSP	0.717/0.692	0.723/0.793
DBF	0.728/0.732	0.715/0.793
SPRH	0.802/0.804	0.824/0.891
BoW	0.841/0.823	0.919/0.958
SPRH+SPRH(d=20)	0.820/0.782	0.883/0.912
SPRH+BoW	0.883/0.875	0.956/0.984

Table 3. The summary of DCG/NN scores

appliance parts. The dataset consists of 362 parts classified into 20 classes and deformable objects such as cables are included. The data was acquired in an automatable process without post-processing by hand. Therefore, it has lots of missing faces caused by occlusions and materials of the parts. In the comparison of existing 3 features, we found that SPRH is the most suitable to classify this dataset. By focusing on small scale local shapes, deformable objects are robustly classified. Further, we have shown that a combination of SPRH for the whole shape and similarity of the local surface patterns improve the result largely.

In this paper, we are interested in to what extent electric appliance parts can be classified based on 3D geometry. As an application, however, using different sensors such as cameras will be effective to classify difficult objects with 3D shape only. Some objects are easily classified using color or texture information. It also helps increase the reliability of the classification.

References

[1] C. B. Akgul, B. Sankur, Y. Yemez, and F. Schmitt. 3d model retrieval using probability density-based shape descriptors. *IEEE Transactions on Pattern Analysis and Machine Intelligence*, 31:1117–1133, 2009.

[2] D. Y. CHEN. On visual similarity based 3d model retrieval. *Proc. Eurographics, 2003*, 2003.

[3] D. Cline, S. Jeschke, A. Razdan, K. White, and P. Wonka. Dart throwing on surfaces. *Computer Graphics Forum*, 28(4):1217–1226, 6 2009.

[4] G. Csurka, C. R. Dance, L. Fan, J. Willamowski, and C. Bray. Visual categorization with bags of keypoints. In *In Workshop on Statistical Learning in Computer Vision, ECCV*, pages 1–22, 2004.

[5] T. Furuya and R. Ohbuchi. Dense sampling and fast encoding for 3d model retrieval using bag-of-visual features. In *CIVR '09: Proceeding of the ACM International Conference on Image and Video Retrieval*, pages 1–8, New York, NY, USA, 2009. ACM.

[6] A. Johnson. *Spin-Images: A Representation for 3-D Surface Matching*. PhD thesis, Robotics Institute, Carnegie Mellon University, Pittsburgh, PA, August 1997.

[7] M. Kazhdan, T. Funkhouser, and S. Rusinkiewicz. Rotation invariant spherical harmonic representation of 3d shape descriptors. In *SGP '03: Proceedings of the 2003 Eurographics/ACM SIGGRAPH symposium on Geometry pro-*

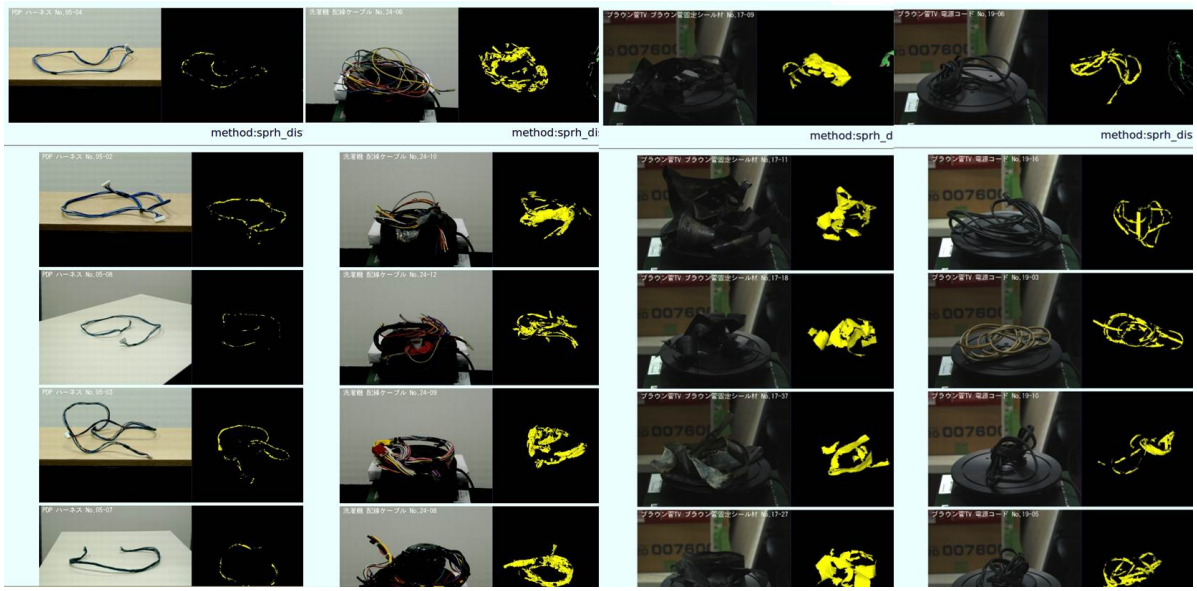

Figure 15. Retrieval results of several deformable objects. The top row is query objects and retrieved objects from the whole dataset are shown below in the order of similarity. Though their configurations differ, they are correctly retrieved.

cessing, pages 156–164, Aire-la-Ville, Switzerland, Switzerland, 2003. Eurographics Association.

[8] X. Li, A. Godil, and A. Wagan. Spatially enhanced bags of words for 3d shape retrieval. In *ISVC '08: Proceedings of the 4th International Symposium on Advances in Visual Computing*, pages 349–358, Berlin, Heidelberg, 2008. Springer-Verlag.

[9] D. Lowe. Object recognition from local scale-invariant features. volume 2, pages 1150 –1157 vol.2, 1999.

[10] P. Papadakis, I. Pratikakis, S. Perantonis, and T. Theoharis. Efficient 3d shape matching and retrieval using a concrete radialized spherical projection representation. *Pattern Recogn.*, 40:2437–2452, September 2007.

[11] R.B.Rusu, Z.C.Marton, N.Blodow, and M.Beetz. Persistent point feature histograms for 3d point clouds. In *Proceedings of the 10th International Conference on Intelligent Autonomous Systems*, 2008.

[12] P. Shilane and T. Funkhouser. Distinctive regions of 3d surfaces. *ACM Trans. Graph.*, 26(2):7, e 07.

[13] P. Shilane, P. Min, M. Kazhdan, and T. Funkhouser. The princeton shape benchmark. In *Shape Modeling International*, June 2004.

[14] D. V. Vranic, D. Saupe, and J. Richter. Tools for 3d-object retrieval: Karhunen-loeve transform and spherical harmonics. In *IEEE MMSP 2001*, pages 293–298, 2001.

[15] E. Wahl, U. Hillenbrand, and G. Hirzinger. Surflet-pair-relation histograms: A statistical 3d-shape representation for rapid classification. *3D Digital Imaging and Modeling, International Conference on*, 0:474, 2003.

[16] K. White, D. Cline, and P. Egbert. Poisson disk point sets by hierarchical dart throwing. pages 129 –132, sep. 2007.

[17] Y. Zhao and G. Karypis. Comparison of agglomerative and partitional document clustering algorithms. *University of Minnesota - Computer Science and Engineering Technical Report*, (02-014), 2002.